Entanglement of mechanical modes in a doubly resonant optomechanical cavity of a correlated emission laser

Mekonnen Bekele [ORCID],[1,2,*] Tewodros Yirgashewa [ORCID],[1] and Sintayehu Tesfa [ORCID][1,3,4]

[1]*Applied Physics Department, Adama Science and Technology University, P.O. Box 1888, Adama, Ethiopia*
[2]*Physics Department, Bule Hora University, P.O. Box 144, Bule Hora, Ethiopia*
[3]*Physics Department, Jazan University, P.O. Box 114, Jazan, Saudi Arabia*
[4]*Physics Department, Addis Ababa University, P.O. Box 1176, Addis Ababa, Ethiopia*

We explore the extent of the induced entanglement of the mechanical modes that can be attributed to the transfer of coherence from two-mode cavity radiation in a doubly resonant optomechanical cavity. It is expected that this scheme can support a generation of mechanical oscillations with a robust degree of entanglement combined with significant controllability. The entanglement is found to be sensitive to the specific choices of the frequencies of the bichromatic drive laser. It also turns out that the degree of entanglement would be enhanced with increasing rates of injection of the atoms but with decreasing initial lengths of a doubly resonant cavity and atomic decay rates. In addition, the entanglement is found to behave qualitatively in the same way for the measures of entanglement we have applied. Since the scheme we considered can possibly be implemented with current technology and allows the quantum features of cavity radiation to be accessible for application, we anticipate that it can be utilized in the realization of continuous-variable quantum information processing.

I. INTRODUCTION

Cavity optomechanical systems (COMs) have become the most desirable candidates to generate and exploit continuous-variable (CV) nonclassical motional states of mechanical oscillators, which can be achieved by employing induced optomechanical coupling, which has a direct relation to the frequency of the cavity radiation [1–3]. In this regard, significant effort has been made to generate entangled states in COMs that offer a rich avenue for experimenting with recent quantum technologies, improving our understanding of quantum optics in the macroscopic regime and at the fundamental quantum physics level and leading to the implementation of various applications [4–7]. These states have been detected in two-mode cavity radiations [8], the cavity mode and mechanical mode [9,10], and two mechanical modes [11,12] using the logarithmic negativity. Further studies have also addressed entangled states of hybrid modes as in two-level-atom [13–15] and three-level-atom [16–18] optomechanical systems.

It has also been established that simultaneously emitted correlated photons with different frequencies as in a cascade three-level atomic system can be a source of robust entanglement in a resonant cavity due to the inherent atomic coherence in the upper and lower energy levels induced by initial preparation of a coherent superposition and/or pumping by a strong coherent laser [19–22]. A strong pumping coherent field in a correlated emission laser (CEL) has also been shown to act as an entanglement amplifier owing to the additional atomic coherence induced by the pumping process when all the atoms are initially in the lower energy level [19,20,23]. On the other hand, whether a bichromatic driving laser can be employed for the generation of entanglement in various configurations has been investigated in some theoretical proposals [24–26] and an experimental realization utilized for cooling a macroscopically heavy movable mirror [27].

Different authors have also shown the effects of various parameters on quantum properties in a doubly resonant optomechanical cavity. For instance, Ge *et al.* showed that the degree of entanglement is reduced with increasing temperature of the thermal phonon bath, with smaller input power P, and with high cavity loss for both the mirror pair and the field pair using the logarithmic negativity [16]. Sete and Eleuch found that two movable mirrors are entangled for a wide range of the drive laser's powers as well as the strength of the atomic drive laser, and the degree of entanglement increases with increasing power P of the cavity drive lasers, while the mirror-mirror entanglement is strong against the thermal phonons temperature but substantially more sensitive to the thermal photon temperature [17]. In addition, Zhou *et al.* showed that the frequency of the mirror oscillation and the injected atomic coherence could affect the output entanglement of two-mode fields [18]. More recently, Bekele *et al.* investigated various mechanisms of enhancing the degree of mechanical squeezing emerging from atomic parameters in a scheme similar to what we intend in the present paper [28].

With this in mind, we seek to extend the scope of discussion to the quantification of the degree of entanglement in the quantum states of mechanical oscillators using realistic parameters like those in Table I to make the result accessible for utilization in a wide range of various controllable parameters other than the input laser power and thermal environmental

*[*]mokebekele1997@gmail.com

TABLE I. Experimental values applied as in [38–41] to plot Figs. 2–7 in the standard case.

Parameter	Values and units
Frequencies of a cavity	$\omega_{L_1} = 741.0\pi$ THz,
driving a bichromatic laser	$\omega_{L_2} = 564.0\pi$ THz
Cavity-mode	$\omega_1 = 864.0\pi$ THz,
frequencies	$\omega_2 = 866.0\pi$ THz
Atom-field coupling ($g_1 = g_2$)	$2.0\pi \times 3.00$ MHz
Cavity damping rates	$\kappa_1 = 4.22$ kHz,
	$\kappa_2 = 5.54$ kHz
Mechanical damping rates ($\gamma_{m_1} = \gamma_{m_2}$)	$2\pi \times 60.00$ Hz
Angular frequencies of movable mirrors ($\omega_{m_1} = \omega_{m_2}$)	$2\pi \times 3.00$ MHz
Masses of the mechanical oscillators ($m_1 = m_2$)	145.00 ng
Initial lengths of a	$L_1 = 0.532$ mm,
doubly resonant cavity	$L_2 = 0.405$ mm
Frequencies of atomic energy levels	$\omega_a = 2\pi \times 432.0$ THz,
	$\omega_b = 2\pi \times 864.0$ THz,
	$\omega_c = 2\pi \times 1297.0$ THz,
Rate of atomic injection r_a	1.60 MHz
Atomic decay rates ($\gamma_a = \gamma_b = \gamma_c = \gamma_{ab} = \gamma_{bc} = \gamma_{ac} = \gamma$)	14.50 MHz
Powers of input lasers driving the cavity ($P_1 = P_2$)	30.00 mW
Thermal bath temperatures of movable mirrors ($T_1 = T_2$)	5.00 mK

temperatures in Ref. [17], in particular, its dependence on atomic parameters such as injection rate and decay rate and cavity parameters such as the frequency of a bichromatic drive laser and the initial lengths of doubly resonant cavities. Specifically, instead of using the power of a laser that drives a cavity [17] or employing the general amplitude of an external pumping laser for the atoms as in [23], we exploit the impact of the frequencies of a bichromatic external cavity drive laser on the strength of entanglement of the modes of mechanical oscillators. In this regard, the degree of entanglement is found to be affected by slight changes to the choices of cavity-driving laser frequencies. We also observed an enhanced degree of entanglement in the case of larger atomic injection rates, smaller atomic decay rates, and smaller initial lengths of a doubly resonant cavity.

To attain our objective, we obtain quantum Langevin equations in the adiabatic regime with the help of the master equation for different modes of the system, confining our study to linear analysis and a good cavity limit and employing the field-mirror interaction Hamiltonian. Then the covariance matrix of the mechanical modes is calculated so that the corresponding entanglement can be calculated within the Gaussian approximation.

II. DYNAMICAL EQUATIONS

In this section, we give the main results of the derivation of the interaction Hamiltonian and the corresponding master equation.

A. Interaction Hamiltonian

The system under consideration is shown in Fig. 1; it comprises three-level atoms in a cascade configuration that initially occupy the lower energy level and are pumped by strong external radiation of amplitude χ and frequency ω_p to establish coherence in the upper and lower atomic energy

levels; then, they are injected at a rate r_a into a doubly resonant cavity. Two-mode cavity radiations are also coupled to the vacuum reservoir via a port mirror M_3. The doubly resonant cavity, on the other hand, is driven by two coherent lasers with frequencies ω_{L_1} and ω_{L_2}, and the two cavity radiations that are split by a beam splitter (BS) in the cavity are coupled to their respective movable mirrors via radiation pressure. In this setting, the movable mirrors are treated as quantum-mechanical harmonic oscillators with effective masses m_j and frequencies $\omega_{m_j} (j = 1, 2)$, which may result in nonclassical properties such as entanglement because the emerging coherent correlation can be transferred to mechanical oscillations. The corresponding quantum harmonic oscillators could thus be modeled with their respective thermal baths at equilibrium at temperatures T_1 and T_2, with the annihilation (creation) operator of each vibrational mode $\hat{b}_j$ $(\hat{b}_j^\dagger)$ satisfying the relation $[\hat{b}_j, \hat{b}_j^\dagger] = 1$, with $j = 1, 2$.

For such a system, the Hamiltonian of the system in the interaction picture can be obtained under the rotating-wave approximation. Therefore, the total interaction Hamiltonian with atom field $\hat{H}_I^{(af)}$ [29] and field mirror $\hat{H}_I^{(fm)}$ [4] interaction can be expressed as $\hat{H} = \hat{H}_I^{(af)} + \hat{H}_I^{(fm)}$, with

$$\hat{H}_I^{(af)} = i\hbar g_1(\hat{\sigma}_{ab}\hat{a}_1 - \hat{a}_1^\dagger\hat{\sigma}_{ba}) + i\hbar g_2(\hat{\sigma}_{bc}\hat{a}_2 - \hat{a}_2^\dagger\hat{\sigma}_{cb})$$
$$+ \hbar(\xi_1 + \xi_2)\hat{\sigma}_{aa} + \hbar\xi_2\hat{\sigma}_{bb} + i\hbar\frac{\chi}{2}(\hat{\sigma}_{ac} - \hat{\sigma}_{ca}), \quad (1)$$

$$\hat{H}_I^{(fm)} = \hbar\sum_{j=1}^{2}[\delta\omega_j\hat{a}_j^\dagger\hat{a}_j + i(\epsilon_j\hat{a}_j^\dagger e^{i\delta\omega_j t} - \epsilon_j^*\hat{a}_j e^{-i\delta\omega_j t})]$$
$$+ \hbar\sum_{j=1}^{2}[\omega_{m_j}\hat{b}_j^\dagger\hat{b}_j + G_{0j}\hat{a}_j^\dagger\hat{a}_j(\hat{b}_j^\dagger + \hat{b}_j)]. \quad (2)$$

In Eq. (1), the atomic operators $\hat{\sigma}_{kk} = |k\rangle\langle k|$ for $k = a, b, c$ are represented by $\hat{\sigma}_{ab} = |a\rangle\langle b|$, $\hat{\sigma}_{bc} = |b\rangle\langle c|$, and $\hat{\sigma}_{ac} = |a\rangle\langle c|$ with the frequency ω_k of the kth atomic states. The term
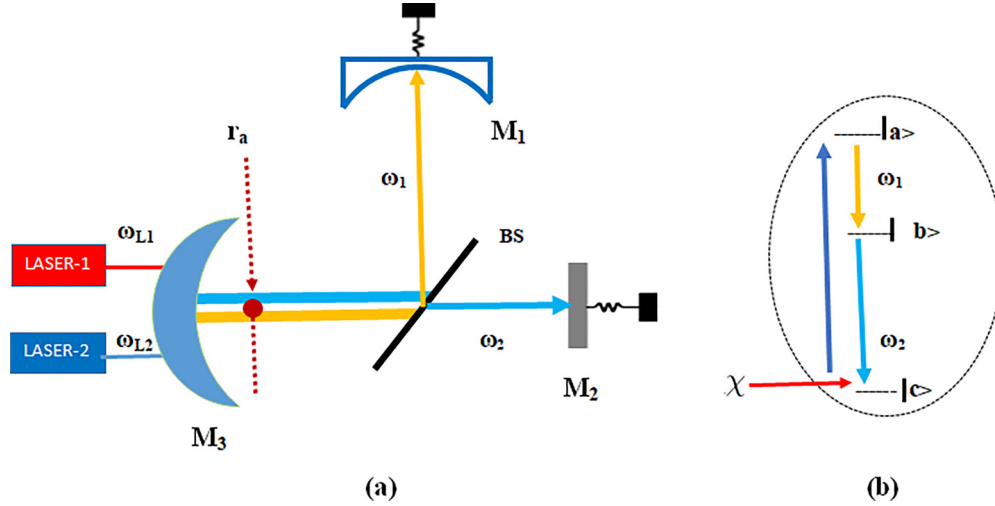
FIG. 1. (a) Schematic representation of a two-mode laser coupled to two movable mirrors, M_1 and M_2. The doubly resonant cavity is driven simultaneously by a physically accessible bichromatic laser of frequencies ω_{L_1} and ω_{L_2}. The two-mode radiations with realistic frequencies ω_1 and ω_2 generated by a three-level atom are filtered by a beam splitter (BS) and are coupled to their respective harmonically oscillating mirrors via radiation pressure. (b) The cascade configuration of a three-level lasing atom that emits two-mode light. An external laser of amplitude χ is applied to generate coherent superposition between the involved atomic energy levels.

g_1 (g_2) expresses the coupling strength between the dipole-allowed atomic transition $|a\rangle \to |b\rangle$ ($|b\rangle \to |c\rangle$) and the two cavity-mode annihilation (creation) operators $\hat{a}_j$ ($\hat{a}_j^\dagger$).

In Eq. (2), the terms $|\epsilon_j| = \sqrt{(\kappa_j P_j)/\hbar\omega_{L_j}}$ and $G_{0_j} = (\omega_j/L_j)\sqrt{\hbar/(m_j\omega_{m_j})}$ ($j = 1, 2$) denote the amplitude of the lasers that drive the cavity and optomechanical coupling rates between the mechanical and cavity fields, respectively, with cavity lengths L_j, decay rates of cavity modes κ_j, input power P_j, and frequencies of the lasers driving the cavity ω_{L_j}. It is also noted that $\xi_1 = \omega_{ab} - \zeta_1$ and $\xi_2 = \omega_{bc} - \zeta_2$, with $\omega_{ab} = \omega_a - \omega_b$ and $\omega_{bc} = \omega_b - \omega_c$ being the frequencies of the $|a\rangle \to |b\rangle$ and $|b\rangle \to |c\rangle$ transitions. Notably, $\zeta_j = \omega_j - \delta\omega_j$ indicates the shifted cavity frequency, and $\delta\omega_j = G_{0_j}\langle\hat{b}_j^\dagger + \hat{b}_j\rangle$ shows the frequency shift due to radiation pressure, while the two-photon resonance is $\omega_p = \zeta_1 + \zeta_2$ and $\delta_j = \zeta_j - \omega_{L_j}$.

B. Master equation

The master equation corresponding to the Hamiltonian in (1) can be obtained by applying the standard approach introduced to study a two-mode three-level laser similar to that in many earlier treatments [29,30]. On the other hand, the mechanical baths that the mechanical oscillators coupled with are considered to be Markovian with a high mechanical Q factor [7]. With these considerations, the master equation for the cavity modes coupled to the vacuum reservoir and the two mechanical oscillator modes coupled to their respective thermal environments takes the form

$$\frac{d}{dt}\hat{\rho}(t) = \alpha_{11}(\hat{\rho}\hat{a}_1\hat{a}_1^\dagger - \hat{a}_1^\dagger\hat{\rho}\hat{a}_1) + \alpha_{11}^*(\hat{a}_1\hat{a}_1^\dagger\hat{\rho} - \hat{a}_1^\dagger\hat{\rho}\hat{a}_1)$$
$$+ \alpha_{22}(\hat{a}_2\hat{\rho}\hat{a}_2^\dagger - \hat{a}_2^\dagger\hat{a}_2\hat{\rho}) + \alpha_{22}^*(\hat{a}_2\hat{\rho}\hat{a}_2^\dagger - \hat{\rho}\hat{a}_2^\dagger\hat{a}_2)$$
$$+ \alpha_{12}(\hat{\rho}\hat{a}_2\hat{a}_1^\dagger - \hat{a}_1^\dagger\hat{\rho}\hat{a}_2^\dagger) + \alpha_{12}^*(\hat{a}_1\hat{a}_2\hat{\rho} - \hat{a}_2\hat{\rho}\hat{a}_1)$$
$$+ \alpha_{21}(\hat{a}_1^\dagger\hat{\rho}\hat{a}_2^\dagger - \hat{a}_2\hat{a}_1^\dagger\hat{\rho}) + \alpha_{21}^*(\hat{a}_2\hat{\rho}\hat{a}_1 - \hat{\rho}\hat{a}_1\hat{a}_2)$$

$$+ \frac{1}{2}\sum_{j=1}^{2} k_j(2\hat{a}_j\hat{\rho}\hat{a}_j^\dagger - \hat{a}_j^\dagger\hat{a}_j\hat{\rho} - \hat{\rho}\hat{a}_j^\dagger\hat{a}_j)$$

$$+ \frac{1}{2}\sum_{j=1}^{2} \gamma_{m_j}[(n_j + 1)(2\hat{b}_j\hat{\rho}\hat{b}_j^\dagger - \hat{b}_j^\dagger\hat{b}_j\hat{\rho} - \hat{\rho}\hat{b}_j^\dagger\hat{b}_j)$$

$$+ n_j(2\hat{b}_j^\dagger\hat{\rho}\hat{b}_j - \hat{b}_j\hat{b}_j^\dagger\hat{\rho} - \hat{\rho}\hat{b}_j\hat{b}_j^\dagger)]. \tag{3}$$

The coefficients α_{ij} are given by

$$\alpha_{11} = -\frac{g_1^2 r_a}{\mathcal{F}}\left[(\gamma_{bc} - i\xi_2)\frac{T_{aa}}{D_2} - \frac{\chi}{2}\frac{T_{ac}^*}{D_1}\right], \tag{4}$$

$$\alpha_{12} = \frac{g_1 g_2 r_a}{\mathcal{F}}\left[(\gamma_{bc} - i\xi_2)\frac{T_{ac}}{D_1} + \frac{\chi}{2}\frac{T_{cc}}{D_2}\right], \tag{5}$$

$$\alpha_{22} = \frac{g_2^2 r_a}{\mathcal{F}}\left[(\gamma_{ab} - i\xi_1)\frac{T_{cc}}{D_2} - \frac{\chi}{2}\frac{T_{ac}^*}{D_1}\right], \tag{6}$$

$$\alpha_{21} = -\frac{g_1 g_2 r_a}{\mathcal{F}}\left[(\gamma_{ab} - i\xi_1)\frac{T_{ac}}{D_1} - \frac{\chi}{2}\frac{T_{aa}}{D_2}\right], \tag{7}$$

with

$$T_{aa} = \frac{1}{2}\chi^2\gamma_{ac}, \quad T_{cc} = \frac{1}{2}[2\gamma_a D_1 + \chi^2\gamma_{ac}],$$

$$T_{ac} = \frac{\chi(T_{cc} - T_{aa})}{2D_2}[\gamma_{ac} - i(\xi_1 + \xi_2)],$$

$$D_1 = \gamma_{ac}^2 + (\xi_1 + \xi_2)^2,$$

$$D_2 = \chi^2\gamma_{ac}\frac{(\gamma_a + \gamma_c)}{2} + \gamma_a\gamma_c[\gamma_{ac}^2 + (\xi_1 + \xi_2)^2],$$

where $\mathcal{F} = \chi^4/4 + (\gamma_{ab} + i\xi_1)(\gamma_{bc} - i\xi_2)$, γ_{ab} and γ_{bc} are dephasing rates for the atomic transitions from $|a\rangle$ to $|b\rangle$ and $|b\rangle$ to $|c\rangle$, γ_j ($j = a, b, c$) is the jth atomic level spontaneous emission decay rate, and γ_{ac} is the two-photon dephasing rate

for atomic transition between the upper and lower energy levels.

Note that κ_j and γ_{m_j} account for the damping of the cavity modes coupled to a vacuum reservoir and the damping rates of the modes of mechanical oscillators coupled to thermal baths at temperatures T_1 and T_2, with the corresponding mean thermal phonon numbers represented by n_1 and n_2. Moreover, n_j ($j = 1, 2$) is represented by $n_j^{-1} = \exp(\hbar\omega_{m_j}/k_B T_j) - 1$, where k_B is the Boltzmann constant and T_j is the temperature of the jth reservoir of the mechanical oscillator.

III. THE QUANTUM LANGEVIN EQUATIONS

After the master equation is applied, the quantum Langevin equations for the atom-cavity mode and optomechanical system can be determined separately in the regime where the atom-field coupling turns out to be much stronger than the optomechanical coupling to analyze the mechanical entanglement [17,18]. With the aid of these equations, we obtain

$$\frac{d\hat{a}_j(t)}{dt} = -\left(\frac{k_j}{2} + \alpha_{jj} + i\delta\omega_j\right)\hat{a}_j(t) - \alpha_{jk}\hat{a}_k^\dagger(t)$$
$$- iG_{0_j}\hat{a}_j(\hat{b}_j^\dagger + \hat{b}_j) + \epsilon_j e^{i\delta_j t} + \hat{F}_j, \quad (8)$$

$$\frac{d\hat{b}_j(t)}{dt} = -\left(\frac{\gamma_{m_j}}{2} + i\omega_{m_j}\right)\hat{b}_j(t) - iG_{0_j}\hat{a}_j^\dagger\hat{a}_j + \sqrt{\gamma_{m_j}}\hat{f}_j, \quad (9)$$

where the terms $\hat{F}_j$ and $\hat{f}_j$ stand for noise operators due to the coupling of the vacuum reservoir with the cavity modes and thermal reservoirs coupled to mechanical oscillators [31].

The correlation properties of the noise operators can be obtained by using Einstein relations: $2\langle D_{\hat{A}\hat{B}}\rangle = \frac{d}{dt}\langle\hat{A}\hat{B}\rangle - \langle(\frac{\hat{A}}{dt} - \hat{F}_A)\hat{B}\rangle - \langle\hat{A}(\frac{\hat{B}}{dt} - \hat{F}_B)\rangle$, where $\langle D_{\hat{A}\hat{B}}\rangle$ is the diffusion coefficient for any operators $\hat{A}$ and $\hat{B} = (\hat{a}_j, \hat{b}_j)$ ($j = 1, 2$) and $\hat{F}_A$ and $\hat{F}_B$ belong to their corresponding noise operators [31]. Using this relation, the equations for the second-order moments of the cavity-mode operators $\hat{a}_j$, and $\langle\hat{F}_{\hat{A}}(t)\hat{F}_{\hat{B}}(t')\rangle = 2\langle D_{\hat{A}\hat{B}}\rangle\delta(t - t')$, the nonzero correlation properties for the noise operators of the vacuum reservoir coupled to the cavity mode are found to be

$$\langle\hat{F}_1^\dagger(t)\hat{F}_1(t')\rangle = -2\,\mathrm{Re}(\alpha_{11})\delta(t - t'), \quad (10)$$

$$\langle\hat{F}_1(t)\hat{F}_1^\dagger(t')\rangle = \kappa_1\delta(t - t'), \quad (11)$$

$$\langle\hat{F}_2(t)\hat{F}_2^\dagger(t')\rangle = [\kappa_2 + 2\,\mathrm{Re}(\alpha_{22})]\delta(t - t'), \quad (12)$$

$$\langle\hat{F}_1^\dagger(t)\hat{F}_2^\dagger(t')\rangle = (\alpha_{12}^* - \alpha_{21}^*)\delta(t - t'), \quad (13)$$

$$\langle\hat{F}_2(t)\hat{F}_1(t')\rangle = \langle\hat{F}_1^\dagger(t)\hat{F}_2^\dagger(t')\rangle^* = -\langle\hat{F}_2^\dagger(t)\hat{F}_1^\dagger(t')\rangle^*$$
$$= (\alpha_{12} - \alpha_{21})\delta(t - t'). \quad (14)$$

In the same manner, the nonvanishing correlations between the mechanical noise operators with the use of Eqs. (2) and (3) can be written in the form

$$\langle\hat{f}_j^\dagger(t)\hat{f}_j(t')\rangle = n_j\delta(t - t'), \quad (15)$$

$$\langle\hat{f}_j(t)\hat{f}_j^\dagger(t')\rangle = (n_j + 1)\delta(t - t'). \quad (16)$$

A. Linearization of quantum Langevin equations

Nonlinearity in Eqs. (8) and (9) means they are not easy to analyze. However, we can overcome this difficulty using the linearization approach [32,33] by assuming that each operator in the system can be written as the sum of its steady-state mean value and a small fluctuation around the steady state:

$$\hat{a}_j = \langle a_j\rangle + \delta\hat{a}_j, \quad \hat{b}_j = \langle b_j\rangle + \delta\hat{b}_j. \quad (17)$$

The parameters $\langle a_j\rangle$ and $\langle b_j\rangle$ are the solutions of the nonlinear algebraic equations obtained using a transformed frame defined by $\tilde{a}_j = \hat{a}_j\exp(-i\delta_j t)$, then factorizing the steady-state component of Eqs. (8) and (9) in the regime of the rotating-wave approximation, and setting the time derivatives to zero:

$$\langle\tilde{a}_j\rangle = \frac{2\epsilon_j}{\kappa_j + 2\alpha_{jj} - 2i\Delta_j}, \quad \langle\hat{b}_j^\dagger + \hat{b}_j\rangle = -\frac{8\omega_{m_j}G_{0_j}\langle\tilde{a}_j^\dagger\tilde{a}_j\rangle}{\gamma_{m_j}^2 + 4\omega_{m_j}^2}, \quad (18)$$

where $\Delta_j = \omega_{L_j} - \omega_j - G_{0_j}\langle\hat{b}_j^\dagger + \hat{b}_j\rangle$ denote the cavity-mode detunings.

On the other hand, a set of linearized differential equations for the fluctuation operators with zero mean can be achieved by introducing the slowly varying fluctuation operators $\delta\hat{a}(t) = \delta\tilde{a}(t)\exp(i\delta_j t)$ and $\delta\hat{b}(t) = \delta\tilde{b}(t)\exp(-i\omega_{m_j}t)$ into Eqs. (8) and (9) and keeping the the coupling terms induced by the two-photon coherence in the absence of the rotating-wave approximation. Then we have

$$\frac{d}{dt}(\delta\hat{a}_j) = -\left(\frac{\kappa_j'}{2} - i\Delta_j\right)\delta\hat{a}_j - \alpha_{jk}\,\delta\hat{a}_k^\dagger + \hat{F}_j$$
$$- iG_{0_j}\langle\tilde{a}_j\rangle(\delta\tilde{b}_j^\dagger e^{i(\delta_j+\omega_{m_j})t} + \delta\tilde{b}_j e^{i(\delta_j-\omega_{m_j})t}), \quad (19)$$

$$\frac{d}{dt}(\delta\tilde{b}_j) = -\frac{\gamma_{m_j}}{2}\delta\tilde{b}_j - iG_{0_j}\langle\tilde{a}_j^\dagger\rangle\delta\hat{a}_j\,e^{-i(\delta_j-\omega_{m_j})t}$$
$$- iG_{0_j}\langle\tilde{a}_j\rangle\delta\hat{a}_j^\dagger\,e^{i(\delta_j+\omega_{m_j})t} + \sqrt{\gamma_{m_j}}\tilde{f}_j, \quad (20)$$

with $\kappa_j' = \kappa_j + 2\alpha_{jj}$, $\tilde{f}_j = \hat{f}_j\exp(i\omega_{m_j}t)$, and $\tilde{F}_j = \hat{F}_j\exp(-i\delta_j t)$. It can be shown that the operators $\delta\hat{a}_j$ and $\delta\hat{b}_j$ satisfy the usual boson commutation relations.

Here, the optomechanical interaction describes parametric amplification, which can be used to realize optomechanical squeezing when $\delta_j = \omega_{m_j}$ [7], whereas the interaction is relevant in inducing quantum state transfer and cooling when $\delta_j = -\omega_{m_j}$ [7,34].

Since we are interested in transferring the entanglement of the cavity fields to the mechanical modes, in this paper, we employ $\delta_j = -\omega_{m_j}$. We also choose $\omega_{L_j} \approx \omega_j + G_{0_j}\langle\hat{b}_j^\dagger + \hat{b}_j\rangle$, so that α_{jj} and α_{jk} are real. Upon adiabatically approximating Eq. (19), we obtain coupled Langevin equations for mechanical oscillators $\delta\tilde{b}_j$,

$$\frac{d(\delta\tilde{b}_1)}{dt} = -\frac{A_1}{2}\delta\tilde{b}_1 - G_{12}\delta\tilde{b}_2^\dagger - r_1\hat{F}_1^\dagger + r_2\hat{F}_2 + \sqrt{\gamma_{m_1}}\tilde{f}_1, \quad (21)$$

$$\frac{d(\delta\tilde{b}_2)}{dt} = -\frac{A_2}{2}\delta\tilde{b}_2 - G_{21}\delta\tilde{b}_1^\dagger + s_1\hat{F}_1 - s_2\hat{F}_2^\dagger + \sqrt{\gamma_{m_2}}\tilde{f}_2, \quad (22)$$

where $A_1 = \gamma_{m_1} - A_{b_1}$ and $A_2 = \gamma_{m_2} - A_{b_2}$, with $A_{b_1} = 4G_1 G_1^* \kappa_2'/K$ and $A_{b_2} = 4G_2 G_2^* \kappa_1'/K$, where $K = \kappa_1' \kappa_2' - 4\alpha_{12}\alpha_{21}$ denotes the effective damping rates for the mechanical modes induced by the radiation pressure. In the same way, $G_{12} = 4G_1 G_2 \alpha_{12}^*/K$ and $G_{21} = 4G_1 G_2 \alpha_{21}^*/K$ are effective couplings between the two mechanical modes induced by the laser system, whereas $r_1 = 2G_1 \kappa_2'/K$, $r_2 = 4G_2 \alpha_{12}^*/K$, $s_1 = 4G_2 \alpha_{21}^*/K$, and $s_2 = 2G_2 \kappa_1'/K$, where many-photon coupling is denoted by $G_j = iG_{0_j}\langle \tilde{a}_j \rangle$.

B. Covariance matrix at steady state

It turns out that the mechanical modes form a bipartite CV system. In this section, we are interested in the properties of its steady state, which, due to the linearized treatment and to the Gaussian nature of the noise operators, is a zero-mean Gaussian state, completely characterized by its symmetrized covariance matrix (CM), which is given by a 4×4 matrix with elements

$$V_{ij_{ss}} = \frac{\langle \mathbf{J}_i \mathbf{J}_j + \mathbf{J}_j \mathbf{J}_i \rangle_{ss}}{2},$$

where $\mathbf{J}_{i_{ss}}$ is the asymptotic value of the ith component of the vector of quadrature fluctuations

$$\mathbf{J}(t) = (\delta\tilde{H}_1, \delta\tilde{L}_1, \delta\tilde{H}_2, \delta\tilde{L}_2)^T,$$

with $\delta\tilde{H}_j = (\delta\tilde{b}_j^\dagger + \delta\tilde{b}_j)/\sqrt{2}$ and $\delta\tilde{L}_j = (\delta\tilde{b}_j - \delta\tilde{b}_j^\dagger)/i\sqrt{2}$. Therefore, the steady-state values are readily calculated using equations of motion (21) and (22), from which we get the matrix equation

$$\dot{\mathbf{J}}(t) = \mathcal{M}\ \mathbf{J}(t) + \mathbf{u}(t), \tag{23}$$

with $\mathcal{M}$ being the drift matrix,

$$\mathcal{M} = \begin{pmatrix} -\frac{A_1}{2} & 0 & -G_{12} & 0 \\ 0 & -\frac{A_1}{2} & 0 & G_{12} \\ -G_{21} & 0 & -\frac{A_2}{2} & 0 \\ 0 & G_{21} & 0 & -\frac{A_2}{2} \end{pmatrix},$$

and $\mathbf{u}(t)$ being a noise vector that contains the noise operators of both the cavity and mirrors,

$$\mathbf{u}(t) = \left(\delta\hat{H}_1^{\text{in}}, \delta\hat{L}_1^{\text{in}}, \delta\hat{H}_2^{\text{in}}, \delta\hat{L}_2^{\text{in}} \right)^T,$$

where the Hermitian input noise operators are $\delta\hat{H}_j^{\text{in}} = (\tilde{F}_{b_j}^\dagger + \tilde{F}_{b_j})/\sqrt{2}$ and $\delta\hat{L}_j^{\text{in}} = (\tilde{F}_{b_j} - \tilde{F}_{b_j}^\dagger)/i\sqrt{2}$, with $\tilde{F}_{b_1} = -r_1\hat{F}_1^\dagger + r_2\hat{F}_2 + \sqrt{\gamma_{m_1}}\tilde{f}_1$ and $\tilde{F}_{b_2} = s_1\hat{F}_1 - s_2\hat{F}_2^\dagger + \sqrt{\gamma_{m_2}}\tilde{f}_2$.

It turns out that the formal solution of the matrix equation (23) is given by

$$\mathbf{J}(t) = \mathbf{J}(0)e^{Mt} + \int_0^t dt' \mathbf{u}(t - t')\ e^{Mt'}, \tag{24}$$

where $\mathbf{J}(0)$ is the vector of the initial values of the components. For the steady-state solution, we take the limit of Eq. (24) as $t \to \infty$. Since the noises $\hat{F}$ and $\hat{f}$ are δ correlated so that they describe a Markovian process, the steady-state CM can therefore be determined by solving the Lyapunov

equation [3]

$$\mathcal{M} V + V^T \mathcal{M} = -\mathcal{P}, \tag{25}$$

where $\mathcal{P}$ is the 4×4 diffusion matrix which characterizes the noise correlations and is defined by the relation $\mathcal{P}_{ij}\delta(t - t') = [\langle u_i(t)u_j(t') + u_j(t')u_i(t) \rangle]/2$. Using the correlations between noise operators $\hat{F}$ and $\hat{f}$, by considering Appendix B in Ref. [28] with $N = M = 0$, the CM satisfies Eq. (25), and we obtain a stable solution(s) when the eigenvalues of matrix $\mathcal{M}$ are negative on the condition that $A_1 A_2 > 4G_{12}G_{21}$ and under the Routh-Hurwitz criterion [35], and therefore, P can be written as

$$\mathcal{P} = \begin{pmatrix} P_{11} & 0 & P_{13} & P_{14} \\ 0 & P_{11} & P_{14} & -P_{13} \\ P_{13} & P_{14} & P_{33} & 0 \\ P_{14} & -P_{13} & 0 & P_{33} \end{pmatrix}, \tag{26}$$

with

$$P_{11} = r_1^2 \left[\frac{\kappa_1 - 2\alpha_{11}}{2} \right] + r_2^2 \left[\frac{\kappa_2 + 2\alpha_{22}}{2} \right] - r_1 r_2 \left[\frac{\alpha_{12} - \alpha_{21}}{2} \right] + \gamma_{m_1}\left(\frac{2n_1 + 1}{2} \right), \tag{27}$$

$$P_{13} = r_1 s_1 \left[\frac{\kappa_1 - 2\alpha_{11}}{2} \right] - r_2 s_2 \left[\frac{\kappa_2 + 2\alpha_{22}}{2} \right] + \frac{(r_1 s_2 + r_2 s_1)}{2} \left[\frac{\alpha_{12} - \alpha_{21}}{2} \right] + \gamma_{m_1}\left(\frac{2n_1 + 1}{2} \right), \tag{28}$$

$$P_{14} = i\frac{(r_2 s_1 - r_1 s_2)}{2} \left[\frac{\alpha_{21} - \alpha_{12}}{2} \right], \tag{29}$$

$$P_{33} = s_1^2 \left[\frac{\kappa_1 - 2\alpha_{11}}{2} \right] + s_2^2 \left[\frac{\kappa_2 + 2\alpha_{22}}{2} \right] - s_1 s_2 \left[\frac{\alpha_{12} - \alpha_{21}}{2} \right] + \gamma_{m_2}\left(\frac{2n_2 + 1}{2} \right). \tag{30}$$

IV. ENTANGLEMENT OF THE MOVABLE MIRRORS

We are now poised to investigate the degree of entanglement for the bipartite Gaussian state of the oscillating mirrors using different criteria. By definition, a quantum state $\hat{\rho}$ of a bipartite system is said to be entangled (inseparable) if and only if

$$\hat{\rho} \neq \sum_i P_i \hat{\rho}_{i1} \otimes \hat{\rho}_{i2}, \tag{31}$$

where $\hat{\rho}_{i1}$ and $\hat{\rho}_{i2}$ are density operators of modes 1 and 2, with $0 \leqslant P_i \leqslant 1$ satisfying $\sum P_i = 1$. With this in mind, several inseparability criteria for continuous-variable product states have been proposed on the basis of different conditions and assumptions. Among these, the quadrature entanglement [36] and the logarithmic negativity [37] are employed, although they mostly render only sufficient conditions. It is therefore compelling to study the relation among various entanglement criteria and to search for prospective conditions under which

this quantum system shows robust movable-mirror entanglement with regard to simultaneously applied bichromatic input lasers which drive the cavity at different frequencies, injected three-level atoms, and altering the initial lengths of a doubly resonant cavity by calculating the elements of the CM when optimal quantum state transfer from the two-mode cavity field to the mechanical modes is considered.

A. Quantification via the sum of quadrature variances

Quantification of entanglement in terms of the sum of quadrature variances is one of the approaches used to verify the entanglement between two mechanical modes [36]. In this respect, a maximally entangled continuous-variable state can be expressed as a coeigenstate of a pair of Einstein-Podolsky-Rosen (EPR)-like operators $\hat{u}$ and $\hat{v}$, and the quantum states of the system are entangled provided that the sum of the variances satisfies the inequality [20]

$$\Delta u^2 + \Delta v^2 < 2, \tag{32}$$

where

$$\hat{u} = \delta\tilde{H}_1 + \delta\tilde{H}_2, \quad \hat{v} = \delta\tilde{L}_1 - \delta\tilde{L}_2, \tag{33}$$

with

$$\delta\tilde{H}_j = \frac{1}{\sqrt{2}}(\delta\tilde{b}_j + \delta\tilde{b}_j^\dagger), \quad \delta\tilde{L}_j = \frac{i}{\sqrt{2}}(\delta\tilde{b}_j^\dagger - \delta\tilde{b}_j), \tag{34}$$

and $[\delta\tilde{H}_j, \delta\tilde{L}_{j'}] = i\delta_{jj'}$.

With the aid of Eqs. (33) and (34) and the relations $\langle\delta\tilde{H}_j\rangle = \langle\delta\tilde{L}_j\rangle = 0$, we obtain the sum of the variances of EPR-like operators as

$$(\Delta u^2 + \Delta v^2) = (\langle\delta\tilde{H}_1\delta\tilde{H}_1\rangle + \langle\delta\tilde{L}_1\delta\tilde{L}_1\rangle)_{ss}$$
$$+ (\langle\delta\tilde{H}_2\delta\tilde{H}_2\rangle + \langle\delta\tilde{L}_2\delta\tilde{L}_2\rangle)_{ss}$$
$$+ (\langle\delta\tilde{H}_1\delta\tilde{H}_2\rangle + \langle\delta\tilde{H}_2\delta\tilde{H}_1\rangle$$
$$- \langle\delta\tilde{L}_1\delta\tilde{L}_2\rangle - \langle\delta\tilde{L}_2\delta\tilde{L}_1\rangle)_{ss}. \tag{35}$$

Upon substituting the elements of the CM for the correlations on the right side of Eq. (35) from the solution of Eq. (25), we obtain

$$(\Delta u^2 + \Delta v^2)_{ss} = [V_{11} + V_{22} + V_{33} + V_{44}$$
$$+ 2(V_{13} - V_{24})]_{ss}. \tag{36}$$

Even though there is no direct interaction between the movable mirrors, it can be conceived that the quantum behavior of the two-mode laser in a CEL could be transferred to the oscillations of the movable mirrors. As a result, the modes of the mechanical oscillators become entangled due to the effective coupling between the two mechanical modes induced by the laser system.

It is also a well-established fact that the external radiation that pumps a three-level atom induces atomic coherent superposition that can significantly modify the absorption-emission mechanism of atoms which is essentially responsible for a strong dependence of the entanglement properties of the radiation on the amplitude of the driving radiation [23]. Making use of the generated laser, the entanglement of the mechanical modes is found to be induced for a wide range of the amplitude χ of a laser that drives the atom, with
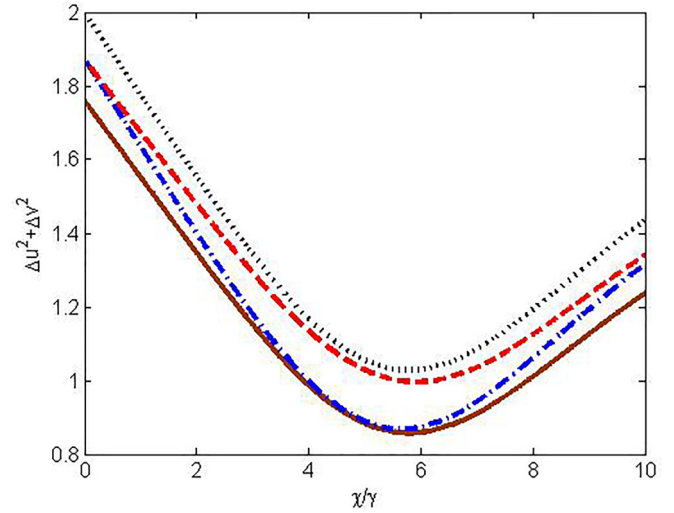

FIG. 2. Plots of $(\Delta u^2 + \Delta v^2)$ against χ/γ at steady state for simultaneously applied two-input lasers driving the cavity with frequencies $\omega_{L_1} = 741.0\pi$ THz and $\omega_{L_2} = 564.0\pi$ THz (brown solid curve), $\omega_{L_1} = \omega_{L_2} = 741.0\pi$ THz (blue dash-dotted curve), $\omega_{L_1} = \omega_{L_2} = 564.0\pi$ THz (red dashed curve), and $\omega_{L_1} = 564.0\pi$ THz and $\omega_{L_2} = 741.0\pi$ THz (black dotted curve). The other parameters are as shown in Table I.

the highest entanglement value appearing at around $\chi \approx 5.75\gamma$. There also exists a minimum strength of the atomic drive laser for which the mechanical-mode entanglement occurs.

In this context, we extend the exploration of the effect of the strength of a bichromatic laser that drives a doubly resonant cavity with regard to the lasers' frequencies, and in Fig. 2, we examine the effect of varying the frequencies of the lasers driving the cavity on the degree of entanglement of the mechanical modes. Particularly, we observe that the degree of mechanical-mode entanglement at steady state as quantified by the sum of quadrature variances $(\Delta u^2 + \Delta v^2)$ is strongest when the frequency of a bichromatic laser ω_{L_1} is greater than that of ω_{L_2}, while the degree of entanglement is found to be weakest when a bichromatic laser's frequency ω_{L_1} is less than ω_{L_2}. In addition, the degree of entanglement is also enhanced but weaker than the strongest one for simultaneously applied equal-frequency input lasers, $\omega_{L_1} = \omega_{L_2} = 741.0\pi$ THz. However, a weaker (better than the weakest) degree of entanglement is observed when the frequencies of a bichromatic laser are small but equal, i.e., $\omega_{L_1} = \omega_{L_2} = 564.0\pi$ THz. This can be explained by the fact that the degree of entanglement is related directly to the effective couplings between the two mechanical modes, G_{12} and G_{21}, so that the entanglement can be enhanced as the effective couplings rely directly on the respective terms α_{12} and α_{21} and on the product G_1G_2. Here, $G_j = iG_{0_j}\langle\tilde{a}_j\rangle$ for $j = 1, 2$, which indicates the many-photon coupling depends directly on the amplitude of a bichromatic laser via $\langle\tilde{a}_j\rangle = 2\epsilon_j/(\kappa_j + 2\alpha_{jj} - 2i\Delta_j)$. These outcomes evince that entanglement is affected by slight changes to the specific choices of the frequencies of the bichromatic drive laser.

In addition, the degree of entanglement of the mechanical modes can be enhanced and controlled by using different
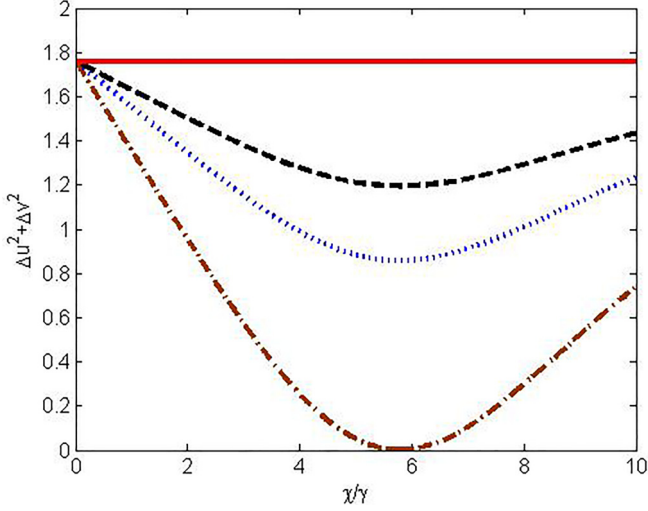
FIG. 3. Plots of $(\Delta u^2 + \Delta v^2)$ against χ/γ at steady state for different atomic injection rates $r_a = 3.12$ MHz (brown dash-dotted curve), $r_a = 1.30$ MHz (blue dotted curve), $r_a = 1.00$ MHz (black dashed curve), and $r_a = 0$ MHz (red solid curve). The other parameters are as shown in Table I.

FIG. 4. Plots of $(\Delta u^2 + \Delta v^2)$ against χ/γ at steady state for different initial lengths of a doubly resonant cavity, $L_1 = 0.426$ mm and $L_2 = 0.324$ mm (blue dash-dotted curve), $L_1 = 0.532$ mm and $L_2 = 0.405$ mm (red solid curve), $L_1 = 0.6384$ mm and $L_2 = 0.486$ mm (black dotted curve), and $L_1 = 0.7448$ mm and $L_2 = 0.567$ mm (brown dashed curve). The other parameters are as shown in Table I.

parameters of three-level atoms, such as atomic injection rates and atomic decay rates. Figure 3 shows that the degree of entanglement would be enhanced at the rate at which atoms are injected into the doubly resonant cavity. In this regard, the increase in atomic injection rate can increase the correlation in the coupled field-mirror modes, which can lead to an enhanced degree of entanglement. In addition, the maximum degree of entanglement is obtained when the atomic injection rate is 3.12 MHz, while very weak entanglement is exhibited when no atoms are injected ($r_a = 0$) into the cavity. On the other hand, a decrease in the initial lengths of a doubly resonant cavity as shown in Fig. 4 is found to enhance the degree of entanglement of the mechanical modes since it increases the field-mirror coupling, which results in an increase in the effective coupling between mechanical modes that appears in direct relation to the correlations in the CM of bipartite mechanical modes. We also note that the optimum degree of entanglement is achieved when the initial lengths of a doubly resonant cavity are $L_1 = 0.426$ mm and $L_2 = 0.324$ mm. This can be described by the fact that the field-mirror couplings G_{0_1} and G_{0_2} through which the transfer of quantum properties from the radiation modes to the mechanical modes has been carried out depend inversely on the respective initial lengths of a doubly resonant cavity.

B. Quantification via logarithmic negativity

Another relevant method which reveals the existence of entanglement in a bipartite state is logarithmic negativity, in which the product density operator for a separable composite state has a positive partial transpose [37]. Notably, the logarithmic negativity for a CV system is defined as
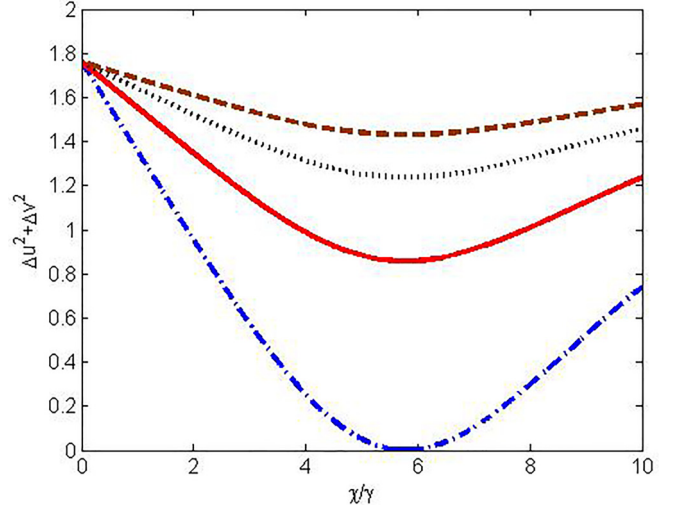
$$E_N = \max[0, -\ln(2V_s)], \qquad (37)$$

where V_s is the smallest eigenvalue of the symplectic matrix [42]. In line with this, the two mechanical modes are said to be entangled if and only if $E_N > 0$ or $V_s < \frac{1}{2}$. In this regard, the smallest symplectic eigenvalue V_s of the partial transpose of the 4×4 correlation matrix is found to have the form

$$V_s = \left(\frac{\sigma - (\sigma^2 - 4\det V)^{\frac{1}{2}}}{2} \right)^{1/2}, \qquad (38)$$

with $\sigma \equiv \det V_A + \det V_B - 2\det V_C$,

$$V = \begin{pmatrix} V_A & V_C \\ V_C^T & V_B \end{pmatrix},$$

$V_A = \mathrm{diag}(V_{11}, V_{22})$, $V_B = \mathrm{diag}(V_{33}, V_{44})$, and

$$V_C = \begin{pmatrix} V_{13} & V_{14} \\ V_{23} & V_{24} \end{pmatrix}.$$

Here, V_A and V_B are the 2×2 block form of covariance matrices that describe each of the mechanical modes separately, while V_C represents the 2×2 matrix of correlations between the mechanical modes.

In the following, the smallest eigenvalue of the symplectic matrix V_s at steady state is plotted against χ/γ by employing Eq. (38). As we can see from Fig. 5, the degree of two-mode mechanical entanglement is altered in a way similar to those presented in Fig. 2 for variations in the frequency combinations of a bichromatic laser; nonetheless, the two different measures of entanglement originate from different sources. On the other hand, we can see from Fig. 6 that the effect of varying the atomic decay rate depends strongly on the value of χ/γ. For $\chi/\gamma < 4$, different atomic decay rates lead to the same entanglement, but for $\chi/\gamma > 4$, lower atomic decay enhances the entanglement.
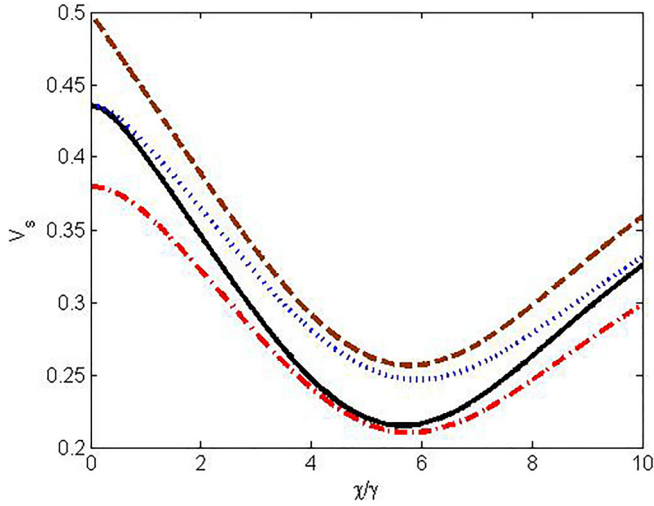
FIG. 5. Plots of V_s against χ/γ at steady state for simultaneously applied two-input lasers driving the cavity with frequencies $\omega_{L_1} = 741.0\pi$ THz and $\omega_{L_2} = 564.0\pi$ THz (red dash-dotted curve), $\omega_{L_1} = \omega_{L_2} = 741.0\pi$ THz (black solid curve), $\omega_{L_1} = \omega_{L_2} = 564.0\pi$ THz (blue dotted curve), and $\omega_{L_1} = 564.0\pi$ THz and $\omega_{L_2} = 741.0\pi$ THz (brown dashed curve). The other parameters are as shown in Table I.

Moreover, the degrees of entanglement using the sum of variances of the quadrature operators $(\Delta u^2 + \Delta v^2)$ and smallest eigenvalue of the symplectic matrix V_s can be compared, where $(\Delta u^2 + \Delta v^2)$ is multiplied by 0.5. As shown in Fig. 7, the degree of entanglement of the mechanical modes that can be quantified by using two different criteria changes and becomes stronger almost in similar manner. But the disparity between the two entanglement criteria, that is, in the sum of quadrature variances and the smallest eigenvalue of a sym-
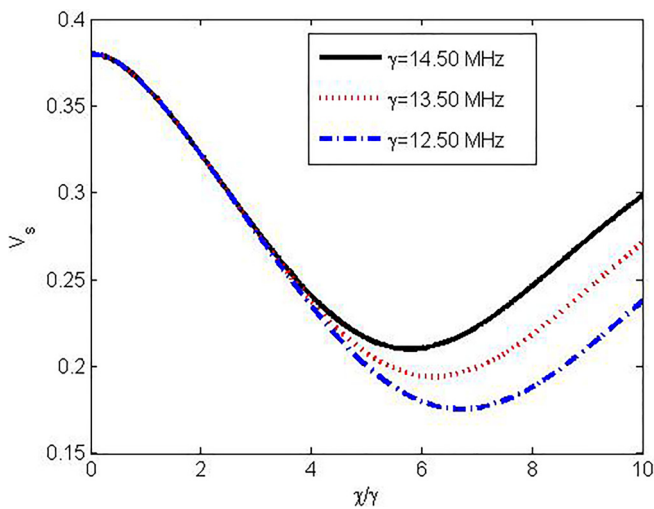

FIG. 6. Plots of V_s against χ/γ at steady state for different atomic decay rates, $\gamma = 14.50$ MHz (black solid curve), $\gamma = 13.50$ MHz (red dotted curve), and $\gamma = 12.50$ MHz (blue dash-dotted curve). The other parameters are as shown in Table I.
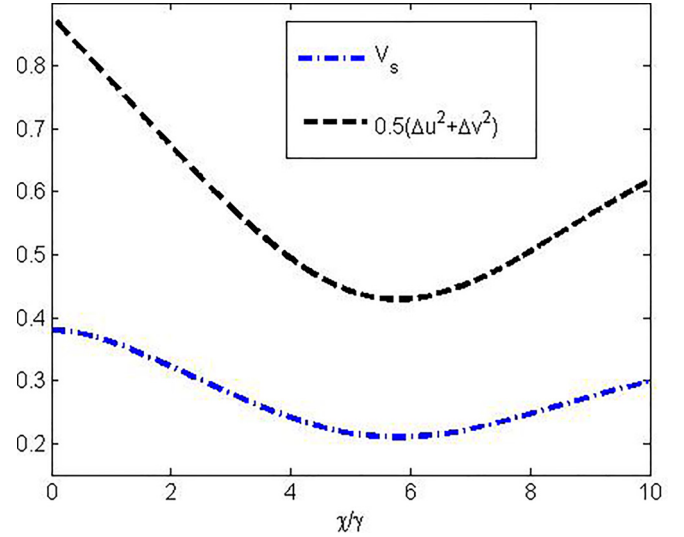

FIG. 7. Plots of $(\Delta u^2 + \Delta v^2)$ and V_s against χ/γ at steady state for the parameters shown in Table I.

plectic matrix, is fundamentally related to the difference in the correlations leading to these phenomena.

V. CONCLUSION

We studied an optomechanical system consisting of two cavity modes coupled to mechanical modes; the cavity modes are driven by lasers and a stream of coherently excited three-level atoms. We showed that entanglement of the mechanical modes can be induced with significant controllability and with potential implementation of the outcome for utilization when the atomic and cavity parameters are involved.

We also found that the entanglement is found to be sensitive to the specific choices of the frequencies of the bichromatic drive laser. This can be described by the fact that the effective couplings between the two mechanical modes can be enhanced because they rely directly on the product of the many-photon coupling that depends directly on the amplitude of a bichromatic laser. Particularly, the generated entanglement can be controlled by adjusting the frequency of the lasers that drive the cavity. It was also clearly shown that the degree of entanglement in the two criteria we employed behave qualitatively in the same way, while the slight disparity between the magnitudes is basically attributed to the variations related to the difference in the correlations leading to these phenomena. In addition, the degree of entanglement was found to be enhanced with an increase in the rates of injection of atoms, smaller initial lengths of a doubly resonant cavity, and smaller atomic decay rates. From the obtained results, we observe that further investigation into inducing other nonclassical correlations between the modes of the mechanical oscillators, such as quantum discord and steering, might be required to fully understand the nature of the transfer of coherent superposition from a correlated emission laser to mechanical oscillators and vice versa.

[1] F. Marquardt, J. P. Chen, A. A. Clerk, and S. M. Girvin, Phys. Rev. Lett. **99**, 093902 (2007).

[2] K. Stannigel, P. Rabl, A. S. Sørensen, P. Zoller, and M. D. Lukin, Phys. Rev. Lett. **105**, 220501 (2010).

[3] L. H. Sun, G. X. Li, and Z. Ficek, Phys. Rev. A **85**, 022327 (2012).

[4] G. S. Agarwal, *Quantum Optics* (Cambridge University Press, New York, 2013).

[5] M. Aspelmeyer, T. J. Kippenberg, and F. Marquardt, *Cavity Optomechanics Nano- and Micromechanical Resonators Interacting with Light* (Springer, Berlin, 2014).

[6] P. Meystre, Ann. Phys. (Berlin, Ger.) **525**, 215 (2013).

[7] M. Aspelmeyer, T. J. Kippenberg, and F. Marquardt, Rev. Mod. Phys. **86**, 1391 (2014).

[8] R. G. Yang, N. Li, J. Zhang, J. Li, and T. C. Zhang, J. Phys. B **50**, 085502 (2017).

[9] M. Paternostro, D. Vitali, S. Gigan, M. S. Kim, C. Brukner, J. Eisert, and M. Aspelmeyer, Phys. Rev. Lett. **99**, 250401 (2007).

[10] D. Vitali, S. Gigan, A. Ferreira, H. R. Bohm, P. Tombesi, A. Guerreiro, V. Vedral, A. Zeilinger, and M. Aspelmeyer, Phys. Rev. Lett. **98**, 030405 (2007).

[11] J. Li, I. M. Haghighi, N. Malossi, S. Zippilli, and D. Vitali, New J. Phys. **17**, 103037 (2015).

[12] P. Neveu, J. Clarke, M. R. Vanner, and E. Verhagen, New J. Phys. **23**, 023026 (2021).

[13] C. Genes, D. Vitali, and P. Tombesi, Phys. Rev. A **77**, 050307(R) (2008).

[14] B. Rogers, M. Paternostro, G. M. Palma, and G. De Chiara, Phys. Rev. A **86**, 042323 (2012).

[15] Q. He and Z. Ficek, Phys. Rev. A **89**, 022332 (2014).

[16] W. Ge, M. Al-Amri, H. Nha, and M. S. Zubairy, Phys. Rev. A **88**, 022338 (2013).

[17] E. A. Sete and H. Eleuch, J. Opt. Soc. Am. B **32**, 971 (2015).

[18] L. Zhou, Y. Han, J. Jing, and W. Zhang, Phys. Rev. A **83**, 052117 (2011).

[19] H. Xiong, M. O. Scully, and M. S. Zubairy, Phys. Rev. Lett. **94**, 023601 (2005).

[20] S. Tesfa, Phys. Rev. A **74**, 043816 (2006).

[21] S. Tesfa, Phys. Rev. A **79**, 063815 (2009).

[22] N. A. Ansari, Phys. Rev. A **48**, 4686 (1993).

[23] S. Tesfa, J. Phys. B **41**, 145501 (2008).

[24] C. Wipf, T. Corbitt, Y. Chen, and N. Mavalvala, New J. Phys. **10**, 095017 (2008).

[25] V. Giovannetti, S. Mancini, and P. Tombesi, Europhys. Lett. **54**, 559 (2001).

[26] V. Giovannetti and D. Vitali, Phys. Rev. A **63**, 023812 (2001).

[27] T. Corbitt, Y. Chen, E. Innerhofer, H. Müller-Ebhardt, D. Ottaway, H. Rehbein, D. Sigg, S. Whitcomb, C. Wipf, and N. Mavalvala, Phys. Rev. Lett. **98**, 150802 (2007).

[28] M. Bekele, T. Yirgashewa, and S. Tesfa, Phys. Rev. A **105**, 053502 (2022).

[29] M. O. Scully and M. S. Zubairy, *Quantum Optics* (Cambridge University Press, Cambridge, 1997).

[30] S. Tesfa, *Quantum Optical Processes: From Basics to Applications* (Springer, Berlin, 2020).

[31] D. F. Walls and G. J. Milburn, *Quantum Optics* (Springer, Berlin, 2008).

[32] S. Chaturvedi, K. Dechoum, and P. D. Drummond, Phys. Rev. A **65**, 033805 (2002).

[33] S. Tesfa, J. Phys. B **41**, 065506 (2008).

[34] M. Pinard, A. Dantan, D. Vitali, O. Arcizet, T. Briant, and A. Heidmann, Europhys. Lett. **72**, 747 (2005).

[35] A. Hurwitz, in *Selected Papers on Mathematical Trends in Control Theory*, edited by R. Bellman and R. Kalaba (Dover, New York, 1964), pp. 70–82.

[36] L. M. Duan, G. Giedke, J. I. Cirac, and P. Zoller, Phys. Rev. Lett. **84**, 2722 (2000).

[37] G. Vidal and R. F. Werner, Phys. Rev. A **65**, 032314 (2002).

[38] W. Luhs and B. Wellegehausen, OSA Continuum **2**, 184 (2019).

[39] O. Arcizet, P. F. Cohadon, T. Briant, M. Pinard, and A. Heidmann, Nature (London) **444**, 71 (2006).

[40] S. Groblacher, K. Hammerer, M. R. Vanner, and M. Aspelmeyer, Nature (London) **460**, 724 (2009).

[41] E. Verhagen, S. Deleglise, S. Weis, A. Schliesser, and T. J. Kippenberg, Nature (London) **482**, 63 (2012).

[42] G. Adesso, A. Serafini, and F. Illuminati, Phys. Rev. A **70**, 022318 (2004).